Hindawi
Journal of Nanomaterials
Volume 2018, Article ID 1519480, 9 pages
https://doi.org/10.1155/2018/1519480

Research Article

Evaluation of Long-Term Inflammatory Responses after Implantation of a Novel Fully Bioabsorbable Scaffold Composed of Poly-L-lactic Acid and Amorphous Calcium Phosphate Nanoparticles

Gaoke Feng,[1] **Thanh Dinh Nguyen**,[1] **Xin Yi**,[1] **Yongnan Lyu**,[1] **Zhiyuan Lan**,[2,3] **Jinggang Xia**,[4] **Tim Wu**,[2,3,5] **and Xuejun Jiang**[1]

[1]*Department of Cardiology, Renmin Hospital of Wuhan University, Wuhan 430060, China*
[2]*VasoTech Inc., Lowell, 600 Suffolk St, Lowell, MA 01854, USA*
[3]*Department of Cardiology, Xuanwu Hospital, Capital Medical University, Beijing 100053, China*
[4]*Department of Plastic Engineering, University of Massachusetts Lowell, Lowell, MA 01854, USA*
[5]*Dongguan TT Medical Inc., Dongguan 523808, China*

Correspondence should be addressed to Gaoke Feng; 123fgk@163.com and Xuejun Jiang; xjjiang@tom.com

Received 3 April 2018; Accepted 14 September 2018; Published 25 November 2018

Academic Editor: Yasuhiko Hayashi

Objectives. Our previous studies have confirmed the superior biocompatibility of the poly-L-lactic acid/amorphous calcium phosphate (PLLA/ACP) scaffolds compared to PLLA scaffolds at 1-month. In the present study, the long-term inflammatory responses of PLLA/ACP scaffolds in a porcine coronary model have been explored. *Methods*. The 24 PLLA scaffolds and 24 PLLA/ACP scaffolds were implanted into the coronary arteries of 24 miniature pigs. Serum levels of ALT, AST, and CRP were measured before operation, as well as 1-month, 6-months, 12-months, and 24-months. The vascular segments were taken for pathomorphological observation. HE staining was used for the inflammatory score and fibrosis score. Immunohistochemical staining detected positive expression indexes of MMP-9 and NF-κB. The expression of inflammation-related proteins of IL-1 and IL-6 was detected by Western Blot in surrounding tissues of scaffolds. *Results*. There was no significant difference between the two groups in ALT, AST, and UR at different time points ($P < 0.05$). The inflammation score in the PLLA/ACP group was lower than that in the PLLA group at 6-months, 12-months, and 24-months ($P < 0.05$), and the fibrosis score was reduced in the PLLA/ACP group than that in the PLLA group at 12-months and 24-months ($P < 0.05$). The expression of MMP-9 and NF-κB in the PLLA/ACP group was significantly less than that in the PLLA group at 6-months, 12-months, and 24-months ($P < 0.05$). The protein expression of IL-1 in the PLLA/ACP group was decreased than that in the PLLA group at 12-months and 24-months ($P < 0.05$). Furthermore, the protein expression of IL-1 was significantly lower than that in the PLLA group at 6-months, 12-months, and 24-months ($P < 0.01$). *Conclusions*. The supplement of ACP nanoparticles can effectively reduce the long-term inflammatory reaction caused by PLLA and has good safety and biocompatibility. The novel bioabsorbable PLLA/ACP scaffold provides reliable guidance for the development and clinical application of bioabsorbable scaffolds in the future.

1. Introduction

The fully bioabsorbable scaffold (FBS) is known as the fourth revolution in the intervention history of coronary heart diseases, and it has multiple advantages with its complete degradation [1]. At present, the research of bioabsorbable scaffold composites focuses mainly on poly-L-lactic acid (PLLA) composites, such as Absorb scaffold developed by Abbott Company in USA, Igaki scaffold in Japanese [2], Xinsorb scaffold in China [3], and MeRes scaffold in India [4]. All of these scaffolds are made of single PLLA material. Although PLLA can be degraded and has certain supporting

performance, its supporting performance is still poor than that of metal scaffolds due to its own limitations. Simultaneously, the lactic acid metabolites produced during the degradation of the PLLA composite will cause long-term chronic stimulation to the vascular tissues around the scaffold, which will induce and aggravate the inflammatory reaction and delay the healing of blood vessels [5, 6]. In addition, increasingly more advanced thrombus formation and stent restenosis are more challenging for single PLLA scaffold in clinical trials. In the situation, the composite material may be the main solution to solve the problem mentioned above. To be specific, the addition of auxiliary composites in PLLA may not only improve the supporting performance of the scaffold but also reduce the thickness, neutralize acid metabolites in degradation of polylactic acid, and reduce inflammation stimulation to benefit vascular repair, so as to avoid recurrence of thrombosis, stent restenosis, and other adverse events. Numerous studies [7, 8] have shown that on the basis of PLLA scaffold, a small amount of ACP nanocomposite is added to form polymer and bioceramic blend composite, showing good mechanical and biological properties in animal arteries. As a biodegradable ceramic composite, ACP nanocomposite has calcium phosphate minerals and weak characteristics, and it has good hydrophilicity, biocompatibility, and mechanical support, which is being widely used in biological and medical fields [9–11]. However, it is not clear whether the long-term chronic inflammatory reaction caused by PLLA can be alleviated by the implantation of PLLA/ACP scaffolds into the blood vessels. Therefore, PLLA/ACP scaffolds and PLLA scaffolds were implanted into coronary arteries of miniature pigs so as to observe and explore the effect of long-term degradation on the inflammatory response of peripheral blood vessels.

2. Methods

2.1. Scaffold Preparation. PLLA/ACP scaffold preparation: first, the ultrahigh molecular weight PLLA (MW = 250,000 g/mol) and the nanosized ACP (size < 150 nm; Ca/P 1 : 1) were mixed into a low-speed stirrer to form PLLA/ACP (96/2, *w*/*w*) composite materials. The composite was placed in a PLLA/ACP tube formed by extrusion of material from a screw extruder. According to the scaffold design pattern, the tube is automatically and accurately sculpted using femtosecond laser engraving technology to form a scaffold product (all sizes are 3.0 mm in diameter × 13.0 mm in length × 150 μm in thickness). The scaffold is crimped onto the balloon of the rapid exchange balloon dilatation catheter by a special process. The PLLA scaffold (3.0 mm diameter × 13 mm length × 150 μm width) was used for the control group; both the production process and the design of PLLA scaffold is the same as the PLLA/ACP scaffold.

2.2. Animal Preparation and Scaffold Implantation. Twenty-four miniature pigs aged 12–16 months were used in this study. The anesthesia and implantation procedures were described previously [7]. Two relatively straight blood vessel segments were randomly selected from left anterior descending, left circumflex, and right coronary arteries as stenting sites. Each pig was implanted with 2 PLLA/ACP scaffolds or 2 PLLA scaffolds. All the animals received 300 mg of aspirin and 75 mg of Plavix for 3 days prior to the implantation procedure and 100 mg of aspirin and 75 mg of Plavix daily for 6 months postimplantation. The animal study protocol was approved by Institutional Animal Care Committee at Renmin Hospital of Wuhan University. All procedures involving animal use were conformed to the *Guide for the Care and Use of Laboratory Animals* published by the US National Institutes of Health (NIH publication no. 85-23, revised 1996).

Table 1: The peri-strut inflammation score is based on the degree of inflammation and extent of the circumference of the artery involved.

Degree/extent	<1/4	1/4–1/2	>1/2
1	1	1	2
2	1	2	3
3	2	3	3

Degree score: 0 = not present; 1 = scattered inflammatory cells; 2 = small and segmental aggregates of inflammatory cells; 3 = larger aggregates widespread or circumferentially distributed. The extent (<1/4, 1/4–1/2, and >1/2) refers to the portion of the circumference of the artery involved. In general, inflammation scores of 0 and 1 denote excellent local biocompatibility, namely, if neutrophils are not seen. An inflammation score of 2 or 3 may denote a biocompatibility issue, especially if neutrophils or large numbers of lymphocytes are present. Large proportions of eosinophils and lymphocytes may be indicative of a hypersensitivity response (Otsuka, 2015).

2.3. Hematological Examination. Two milliliters of a blood sample was collected from each pig 24 hours prior to the procedure and 1 month, 6 months, 12 months, and 24 months postscaffold implantation. The concentrations of alanine aminotransferase (ALT), aspartate aminotransferase (AST), blood urea nitrogen (BUN), creatinine (Cr), and C-reactive protein (CRP) from each blood sample were measured using an automatic biochemistry analyzer (AU5400, Siemens, Germany) according to the manufacturer's instructions.

2.4. Pathological Examination. A total of 6 miniature pigs were sacrificed in each group at 1 month, 6 months, 12 months, and 24 months. The stented vascular segment was took out to remove vessels and tissues around the scaffold and placed into liquid nitrogen for cryopreservation for following molecular biological detection. Vascular specimens of the scaffold were fixed and embedded with 10% formalin solution. Collected specimens were then divided into five parts: the proximal reference vessel, the proximal stented vessel, the middle stented vessel, the distal stented vessel, and the distal reference vessel. Furthermore, 5 slices of each section were stained with hematoxylin-eosin (HE). Four quadrants of the visual field were taken for each slice under an optical microscope at 40x and 200x magnification. The inflammatory score and the fibrin score were evaluated based on the method mentioned in Tables 1 and 2.

Immunohistochemical staining of MMP-9 and NF-κB was performed with the selection of partial slices. Besides, 4 visual fields were taken for each slice. The percentage of positive cells and mean optical density in the random field

Table 2: The fibrin score is based on the following.

0	No fibrin/fibrinoid deposits present
1	Minimal, spotty, focal fibrin/fibrinoid deposits around the struts and/or throughout the neointima
2	Mild to moderate fibrin/fibrinoid deposits around struts and/or throughout the neointima (small lakes locally bridging between two adjacent struts or widely distributed in coalescing flakes)
3	Heavy fibrin/fibrinoid deposits around the struts, bridging between several adjacent struts and/or throughout the neointima

Fibrin (or fibrinoid deposits) is a normal and expected component of the neointima in the early stages of healing. In the process of organization, the neointima is primarily comprised of fibrin, and the amount decreases as organization progresses. Mature neointima usually contains no to very low levels of residual fibrin. Large amounts of residual fibrin can interfere with long-term stability of the neointima.

of vision was measured by the Image-pro Plus6.0 image analysis system. The positive expression index = percentage of positive cells × mean optical density × 100.

2.5. Western Blot Analysis. The vascular tissues around the scaffolds at each time point were removed from the liquid nitrogen and homogenized in a homogenizer. The homogenates were tested by Western Blot. The gel scanner was used to analyze the quantum intensity of IL-1 and IL-6 electrophoretic bands. Glyceraldehyde-3-phosphate dehydrogenase (GAPDH) was used as an internal control to ensure an equal amount of protein extract in each sample. The ratio of the quantum intensity of electrophoresis bands of IL-1 and IL-6 to the quantum intensity of electrophoretic bands of GAPDH was used as a parameter for the expression levels of IL-1 and IL-6 in muscle tissue.

2.6. Data Representation and Statistical Analysis. All measurements were expressed as mean ± standard deviation (SD). Independent T–tests were performed to detect between-group differences. For multiple comparisons, analysis of variance (ANOVA; with Tukey post hoc comparisons) or the Kruskal-Wallis test (ranks with Dunn's method pairwise) was used as appropriate. All statistical tests were 2-tailed, and a P value < 0.05 was considered statistically significant. Statistical analyses were performed with SPSS 17.0 (Statistical Product and Service Solutions Ltd.).

3. Results

3.1. General Situation of Animals. Twenty-four minipigs were all healthy and survived until the end of each time point. No major adverse cardiovascular events such as stent thrombosis and myocardial infarction occurred. The body weights of the two groups of pigs increased. The weight gain of the PLLA group was 6.37 ± 3.42 kg, and that of the PLLA/ACP group was 6.64 ± 3.85 kg; there was no significant difference between the two groups ($P > 0.05$).

3.2. Hematology Test Results. There were no significant differences in the serum levels of ALT, AST, UR, CR, LDH, and CRP between the two groups at 1, 6, 12, and 24 months after scaffold implantation ($P > 0.05$, Table 3). There was also no statistical significance between the two groups at each time point ($P > 0.05$, Table 3). It was shown that both groups did not cause changes in hematological inflammation after scaffold implantation and did not cause systemic inflammation.

3.3. Pathological Examination. After the sacrifice of experimental animals, heart specimens of all miniature pigs were observed to have no obvious enlargement or scar formation. No other obvious abnormalities, such as infarct, were found in the myocardium of the blood supply area of the coronary artery in each scaffold. In the PLLA group, signs of inflammation were found in 2 scaffolds at 6 months, 3 scaffolds at 12 months, and 4 scaffolds at 24 months (Figure 1). By contrast, only one stented segment showed red and swollen inflammatory reaction signs at 12 months in the PLLA/ACP group. The above results showed that the inflammatory reaction in the PLLA group was more obvious and increased with time.

At 1, 6, 12, and 24 months after scaffold implantation, HE staining in two groups revealed that there was a large number of inflammatory cell infiltration around the scaffold in the PLLA group (Figure 2) and increased with the prolongation of scaffold implantation time. Inflammation scores in surrounding tissues of the scaffold were significantly less in the PLLA/ACP group than that in the PLLA group at 6 months, 12 months, and 24 months ($P < 0.05$, Table 4). The fibrosis results showed that the fibrosis score was much lower in the PLLA/ACP group than that in the PLLA group at 12 months and 24 months ($P < 0.05$, Table 4). It was indicated that the addition of ACP nanocomposite in PLLA scaffold could reduce the chronic inflammatory reaction of PLLA.

Immunohistochemical staining of MMP-9 showed that the positive staining of MMP-9 protein was mainly distributed in the nuclei of inflammatory cells in perivascular tissues, showing brown-yellow granules (Figure 3). Statistical analysis revealed that 6, 12, and 24 months after scaffold implantation, the positive expression index of MMP-9 around the composite was higher in the PLLA group than that in the PLLA/ACP group ($P < 0.05$, Table 5). The expression of MMP-9 in the PLLA group was gradually increasing from 1 month to 24 months ($P < 0.05$, Table 5), but there was no obvious change in each time point in the PLLA/ACP group after operation ($P > 0.05$, Table 5).

Further immunohistochemical staining results indicated that the positive staining of NF-κB protein was mainly distributed in the nuclei of inflammatory cells in the intimal vessels, revealing brown-yellow granules (Figure 4). The results showed that the positive expression index of NF-κB around the composite in the PLLA group was much more than that in the PLLA/ACP group 6, 12, and 24 months after scaffold implantation ($P < 0.05$). Meanwhile, the expression of NF-κB in the PLLA group showed a gradual increasing trend from 1 month to 24 months ($P < 0.05$, Table 3).

Table 3: Coronary artery serum levels of ALT, AST, UR, CR, and CRP.

	Preimplant	1 month	6 months	12 months	24 months
ALT (U/L)					
PLLA	49.17 ± 12.46	61.67 ± 19.98	65.33 ± 18.96	69.17 ± 17.57	64.00 ± 17.80
PLLA/ACP	51.17 ± 15.43	58.00 ± 26.80	71.67 ± 21.60	72.33 ± 24.04	58.83 ± 17.75
P value	0.81	0.79	0.60	0.80	0.63
AST (U/L)					
PLLA	38.33 ± 8.55	49.50 ± 18.92	56.83 ± 16.82	56.50 ± 21.84	54.33 ± 17.11
PLLA/ACP	38.00 ± 8.60	43.67 ± 18.85	60.33 ± 26.45	45.50 ± 28.23	51.33 ± 24.23
P value	0.95	0.60	0.79	0.47	0.81
UR (mmol/l)					
PLLA	5.13 ± 1.32	6.22 ± 1.05	5.77 ± 3.19	6.83 ± 3.02	6.80 ± 3.07
PLLA/ACP	4.50 ± 1.44	5.72 ± 1.72	6.38 ± 2.98	6.28 ± 2.99	7.25 ± 2.88
P value	0.45	0.56	0.74	0.76	0.80
CR (μmol/l)					
PLLA	78.83 ± 13.78	118.67 ± 25.56	92.17 ± 23.03	89.50 ± 28.89	113.17 ± 24.59
PLLA/ACP	84.00 ± 15.21	105.83 ± 23.92	104.33 ± 29.57	102.33 ± 29.84	100.50 ± 26.49
P value	0.55	0.39	0.44	0.47	0.41
LDH (U/l)					
PLLA	177.33 ± 66.01	300.67 ± 157.83	217.50 ± 81.45	193.33 ± 88.80	199.83 ± 120.87
PLLA/ACP	179.50 ± 46.47	243.67 ± 107.07	201.83 ± 35.89	232.33 ± 104.32	278.83 ± 111.24
P value	0.95	0.48	0.68	0.50	0.27
CRP (mg/l)					
PLLA	0.93 ± 0.47	1.64 ± 0.86	1.33 ± 0.53	1.71 ± 0.48	1.10 ± 0.51
PLLA/ACP	1.13 ± 0.44	1.75 ± 0.65	1.62 ± 0.41	1.28 ± 0.43	1.29 ± 0.64
P values	0.47	0.79	0.33	0.14	0.58

Notes: Data are presented as mean ± standard deviation. *P* values: the PLLA/ACP group compared with the PLLA group.

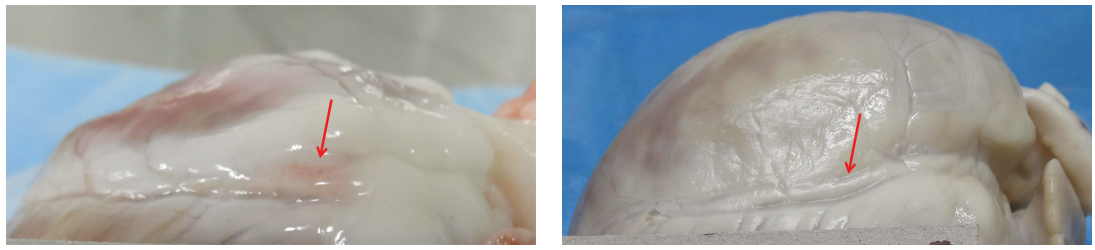

(a) (b)

Figure 1: Gross necropsy examination of the stented hearts. (a) PLLA scaffold. Notable tissue inflammation around the stented segment (red arrow). (b) PLLA/ACP scaffold. There are no coronary abnormalities, epicardial hemorrhage, myocardial infarction, and aneurysms (red arrow).

However, no remarkable change was found in each time point of the PLLA/ACP group after operation ($P > 0.05$, Table 3).

3.4. Western Blot Results. The expression level of IL-1 in the PLLA/ACP group was significantly lower than that of the PLLA group 12 and 24 months after scaffold implantation ($P < 0.05$, Figure 5). There was no significant difference in the level of IL-1 expression among all the detected time points in the PLLA/ACP group after scaffold implantation ($P > 0.05$, Figure 5). Nevertheless, the expression level of IL-1 was evidently higher at 12 and 24 months than 1 month after implantation in the PLLA group ($P < 0.05$, Figure 5). Meanwhile, the expression level of IL-1 was also increased gradually with the prolongation of implantation time.

The expression level of IL-6 was significantly reduced in the PLLA/ACP group than that of the PLLA group 6, 12, and 24 months after scaffold implantation ($P < 0.05$, Figure 5). Furthermore, no significant difference was measured in the level of IL-6 expression at different time points after scaffold implantation in the PLLA/ACP group ($P > 0.05$, Figure 5). At the same time, the expression level

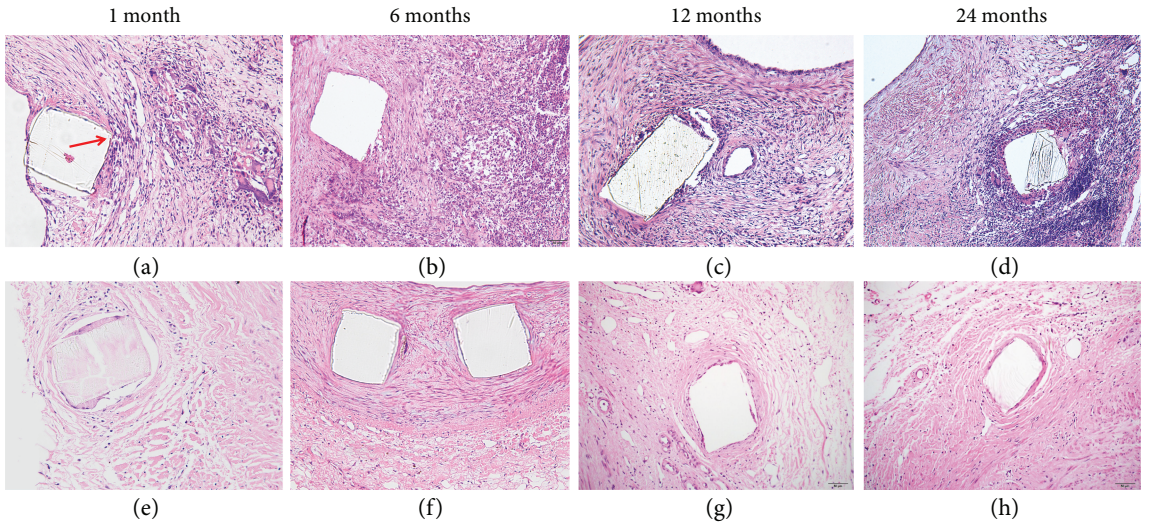

Figure 2: Hematoxylin-eosin staining. Histological cross sections of the stented porcine coronary arteries from 1 month to 24 months (×200): (a–d) PLLA scaffolds and (e–h) PLLA/ACP scaffolds. Note the remarkable vascular wall swelling, tissue inflammation with PLLA scaffold (red arrows).

Table 4: Pathology results.

	1 month	6 months	12 months	24 months
Inflammation score				
PLLA	0.83 ± 0.53	1.3 ± 0.47	1.47 ± 0.68	1.77 ± 0.43
PLLA/ACP	0.63 ± 0.49	0.97 ± 0.61	1.07 ± 0.74	0.93 ± 0.58
P values	0.13	0.02	0.03	<0.01
Fibrin score				
PLLA	0.60 ± 0.62	1.17 ± 0.53	1.47 ± 0.68	1.73 ± 0.58
PLLA/ACP	0.63 ± 0.49	0.96 ± 0.61	1.07 ± 0.64	1.10 ± 0.61
P values	0.82	0.18	0.02	<0.01

Notes: Data are presented as mean ± standard deviation. *P* values: the PLLA/ACP group compared with the PLLA group.

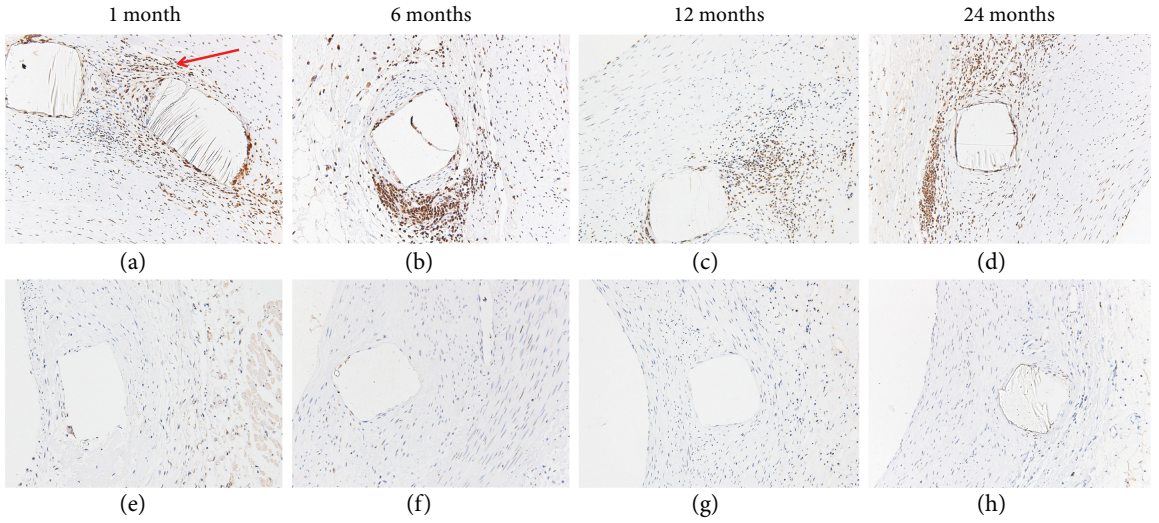

Figure 3: Immunohistochemistry staining of NF-κB: positive cells with the PLLA scaffold (a–d) and with the PLLA/ACP scaffold (e–h). Note the significantly lower expression of NF-κB in the PLLA/ACP stented artery (e–h) compared with that of the PLLA stented artery (a–d). (The red arrows show positive cells. ×200.)

Table 5: Immunohistochemistry results.

	1 month	6 months	12 months	24 months
MMP-9 positive index				
PLLA	8.65 ± 2.65	13.04 ± 4.77	21.13 ± 4.89	29.32 ± 5.89
PLLA/ACP	7.43 ± 2.71	6.94 ± 3.30	9.58 ± 5.58	8.49 ± 4.23
P values	0.18	0.00	0.00	0.00
NF-κB positive index				
PLLA	29.38 ± 3.96	34.44 ± 4.07	40.00 ± 3.19	50.62 ± 5.12
PLLA/ACP	26.51 ± 5.15	30.91 ± 3.42	26.24 ± 4.52	20.29 ± 5.39
P values	0.07	0.02	0.00	0.00

Notes: Data are presented as mean ± standard deviation. *P* values: the PLLA/ACP group compared with the PLLA group.

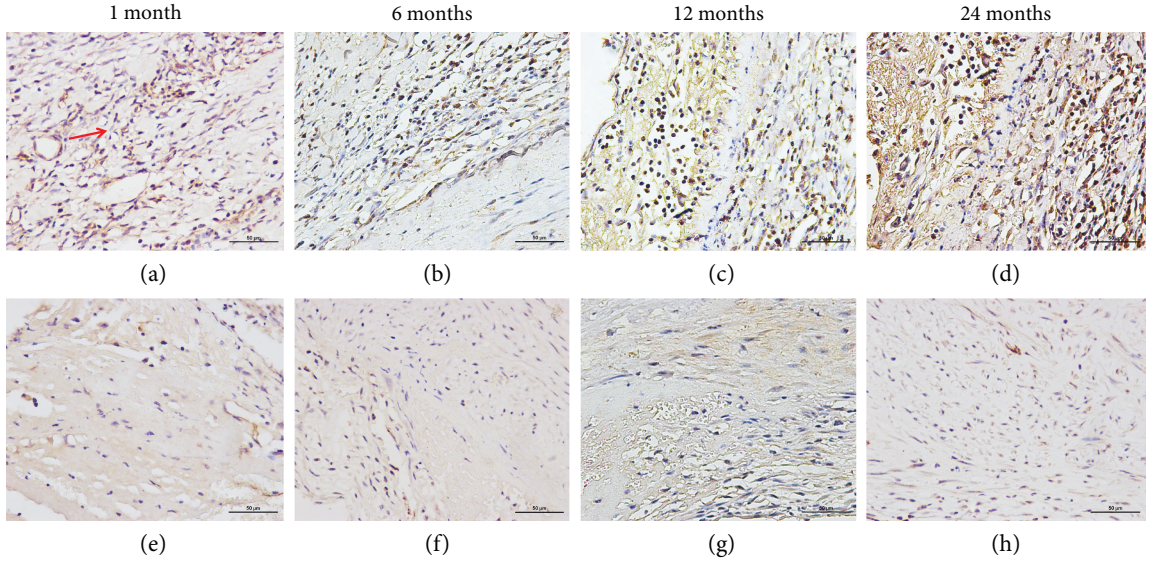

Figure 4: Immunohistochemistry staining of MMP-9: positive cells with the PLLA scaffold (a–d) and with the PLLA/ACP scaffold (e–h). Note the significantly lower expression of MMP-9 in the PLLA/ACP stented artery (e–h) compared with that of the PLLA stented artery (a–d). (The red arrows show positive cells. ×200.)

of IL-6 was evidently higher at 6, 12, and 24 months than 1 month after scaffold implantation in the PLLA group ($P < 0.05$, Figure 5).

4. Discussion

It is known that the inflammatory reaction of vascular tissue plays an extremely important role in the course of the occurrence and development of coronary atherosclerosis. Essentially, coronary atherosclerotic heart disease can actually be considered as an inflammatory disease. Simultaneously, vascular inflammation is also an important cause to promote intima damage, proliferation of smooth muscle, and scaffold thrombosis and restenosis after coronary artery scaffold implantation. Therefore, alleviating or eliminating the inflammatory response after scaffold implantation is a key factor in reducing the incidence of thrombosis and scaffold restenosis after implantation. In our previous experiment [10], a weak alkaline ACP nanoparticle with good hydrophilicity and biocompatibility was added with PLLA to produce a novel bioabsorbable scaffold. To a certain extent, the biocompatibility of PLLA scaffolds was increased accordingly, which accelerated endothelialization of blood vessels and increased radial supporting performance of scaffolds [8]. In this experiment, PLLA scaffolds and PLLA/ACP scaffolds were implanted into the porcine coronary arteries. The effect of PLLA/ACP scaffolds was explored on microinflammatory reaction in blood vessels and surrounding tissues at 1 month, 6 months, 12 months, and 24 months.

Microinflammatory reaction is quite different from traditional inflammatory diseases. It is a chronic slight inflammatory reaction, which is manifested in the infiltration of inflammatory cells and the increase of adhesion molecules, chemokines, proinflammatory cytokines, C-reactive protein, and other inflammation-related proteins [12]. CRP protein is one of the highly sensitive inflammatory markers. It is an acute related protein that can be synthesized and released into the blood when the body is seriously damaged by inflammation. Therefore, the systemic inflammation can be observed through the concentration of CRP in the blood [13]. Additionally, NF-κB is an inflammatory transcription factor that induces the formation of superoxide radical in

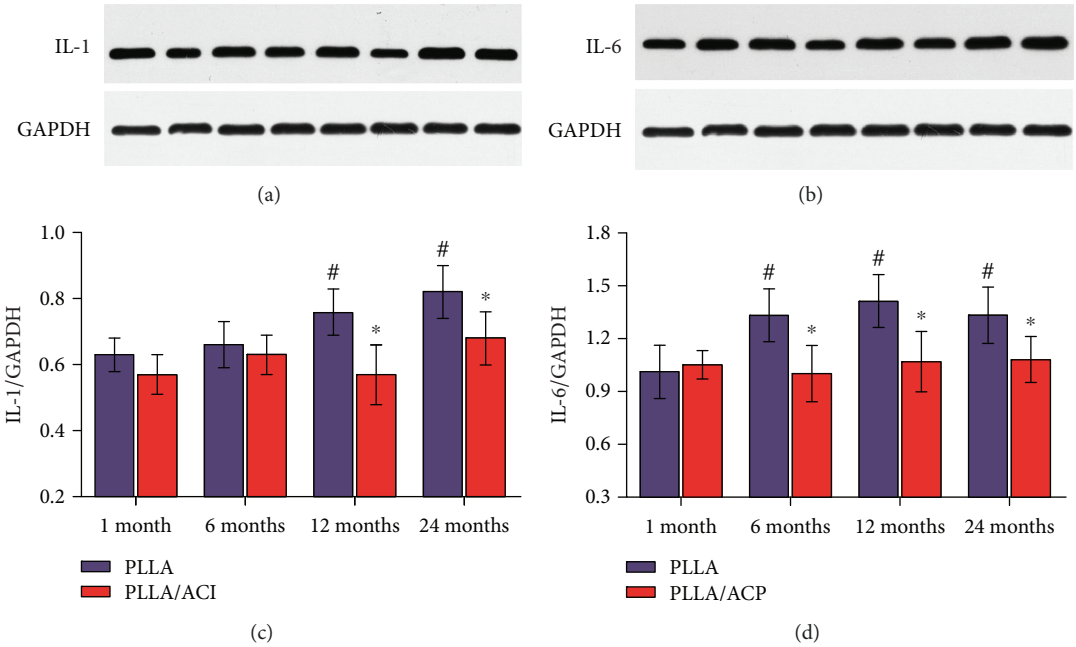

Figure 5: Western Blotting analysis of coronary arteries treated with PLLA scaffolds and PLLA/ACP scaffolds for 24 months. The expression of IL-1 in the PLLA/ACP group was significantly lower than that in the PLLA group at 12 months and 24 months (a and c). The expression of IL-6 in the PLLA/ACP group was significantly lower than that in the PLLA group at 6 months, 12 months, and 24 months (b and d). $^*P < 0.05$ means the PLLA/ACP group compared with the PLLA group.

the body [14], and can also promote the production of other inflammatory factors, such as MMP-9. Consequently, the expression of NF-κB will be enhanced resulted from increased local inflammatory response, indicating the degree of inflammation to some extent. IL-1 and IL-6 are proinflammatory cytokines and have essential effect on acute or chronic inflammation [15]. At the same time, corresponding expression can also activate complement and CRP expression, stimulate neutrophil, endothelial cells, monocyte macrophages and lymphocytes to migrate and extravasate to local tissues, causing inflammatory reaction. In turn, these activated inflammatory cytokines also produce more adhesion molecules, cytokines and chemokines, which further aggravate the inflammatory response. Inflammatory mediators such as IL-1 and IL-6 released at early stage of inflammation can promote the expression of MMP-9, while overexpressed MMP-9 can degrade extracellular matrix, destroy basement membrane, and further infiltrate inflammatory cells into deeper tissues [16]. Moreover, under the action of MMP-9, the extracellular matrix is degraded in the basement membrane, followed by the destroyed integrity of muscle fibers, which result in the infiltration of inflammatory cells into muscle tissue, leading to a series of pathological inflammatory changes, such as necrosis and phagocytosis of muscle fibers. Therefore, the detection NF-κB, MMP-9, IL-1, IL-6 expressions in the vascular tissue around the scaffold can reflect the degree of microinflammatory reaction.

In this study, the inflammatory response in tissues around the scaffold was evaluated by detecting expression levels of IL-1 and IL-6 in homogenate of surrounding tissues of the scaffold, analyzing inflammation score and fibrosis score by histopathological staining, and testing positive expression indexes of MMP-9 and NF-κB with immunohistochemistry. There were more obvious inflammatory reactions in scaffolds of PLLA group via observing general anatomical specimens. Besides, the pathological staining score and the fibrosis score were less in PLLA/ACP group than those in PLLA group. The positive expression index of MMP-9 in PLLA group was significantly higher than that in PLLA/ACP group 6 months, 12 months and 24 months after operation, and showed a gradual increasing trend. Meanwhile, it increased 2 times at 24 months after operation compared with that at 1 month after operation. The NF-κB positive expression index was significantly higher in PLLA group than that in PLLA/ACP group 12 months and 24 months after implantation. At the same time, Western Blot in tissue homogenate revealed that inflammation-related protein IL-1 was obviously higher 12 months and 24 months after implantation, and IL-6 was evidently higher 6 months, 12 months, and 24 months after implantation in the PLLA group when compared to those in the PLLA/ACP group. Besides, the expression level of IL-6 increased with time in the PLLA group. The above results suggested that the inflammatory reaction of the vascular tissue around the scaffold was gradually aggravated with the prolongation of the implantation time in the PLLA scaffold [17].

As for the possible mechanism, it was speculated that the microinflammatory reaction caused by PLLA scaffolds implanted *in vivo* was nonspecific acidic inflammatory reaction, which was induced by acid intermediate metabolite of lactic acid released during PLLA decomposition and degradation. ACP is an amorphous apatite with high solubility and favorable bioabsorbability. Following the addition of ACP with hydrophilic, weakly alkaline and biodegradability,

ACP releases ions into the aqueous medium during hydrolysis, forming potential supersaturated Ca^{2+} and $P_2O_7^{4-}$ ions. The release of $P_2O_7^{4-}$ ions will further hydrolyze and produce OH^- ions. Subsequently, OH^- ions neutralize acidic products gathered during the degradation of PLLA and thus reduce aseptic inflammatory response (antiacid and anti-inflammatory principles, as shown in the following equation). In addition, the combination of Ca^{2+} ions and carboxylic anions to form insoluble salts is another approach for deacidification, which further increases the biocompatibility of PLLA scaffolds.

5. Conclusions

In this study, the inflammatory response to the vascular tissue around the scaffold was gradually increased as the time of implantation was prolonged in PLLA scaffolds. The integration of small-dose ACP nanocomposite could reduce the long-term chronic inflammatory response after the implantation of PLLA scaffolds. The novel bioabsorbable PLLA/ACP scaffold has good biological safety and biocompatibility and is accompanied by slight inflammatory reaction. Therefore, the application of novel bioabsorbable PLLA/ACP scaffold is more optimistic, which can widen new ideas for the development of fully bioabsorbable scaffolds in the future.

6. Limitations

Firstly, there was no atherosclerosis in the coronary artery of the experimental miniature pigs, and its vascular repair might be different from that of the human. Secondly, the relatively small sample size might affect the results of statistical analysis. Our next step is to further expand to the atherosclerotic model and to detect and evaluate the new fully bioabsorbable scaffolds in the model of coronary artery intima damage.

Data Availability

The data used to support the findings of this study are available from the corresponding author upon request.

Conflicts of Interest

The authors have no conflicts to disclose.

Acknowledgments

The study was supported by grants from the Fundamental Research Funds for the Central Universities of China (2042017kf0077), the Wuhan Youth Science and Technology Chenguang Plan (2017050304010280), the Guangdong Innovative and Entrepreneurial Research Team Program (2014ZT05S008), the NSFC Guidance fund project of the Renmin Hospital of Wuhan University (RMYD2018M24).

References

[1] D. G. Rizik, J. B. Hermiller, and D. J. Kereiakes, "The ABSORB bioresorbable vascular scaffold: a novel, fully resorbable drug-eluting stent: current concepts and overview of clinical evidence," *Catheterization and Cardiovascular Interventions*, vol. 86, no. 4, pp. 664–677, 2015.

[2] M. Werner, A. Schmidt, S. Scheinert et al., "Evaluation of the biodegradable Igaki-Tamai scaffold after drug-eluting balloon treatment of de novo superficial femoral artery lesions: the GAIA-DEB study," *Journal of Endovascular Therapy*, vol. 23, no. 1, pp. 92–97, 2016.

[3] X. Lv, L. Shen, Y. Wu et al., "Healing score of the Xinsorb scaffold in the treatment of de novo lesions: 6-month imaging outcomes," *The International Journal of Cardiovascular Imaging*, vol. 34, no. 7, pp. 1009–1016, 2018.

[4] A. Seth, Y. Onuma, R. Costa et al., "First-in-human evaluation of a novel poly-L-lactide based sirolimus-eluting bioresorbable vascular scaffold for the treatment of de novo native coronary artery lesions: MeRes-1 trial," *EuroIntervention*, vol. 13, no. 4, pp. 415–423, 2017.

[5] T. Murakami, S. Otsuki, K. Nakagawa et al., "Establishment of novel meniscal scaffold structures using polyglycolic and poly-L-lactic acids," *Journal of Biomaterials Applications*, vol. 32, no. 2, pp. 150–161, 2017.

[6] J. Chu, S. Zeng, L. Gao et al., "Poly(L-lactic acid) porous scaffold-supported alginate hydrogel with improved mechanical properties and biocompatibility," *The International Journal of Artificial Organs*, vol. 39, no. 8, pp. 435–443, 2016.

[7] G. Feng, J. Xiao, Y. Bi et al., "12-month coronary angiography, intravascular ultrasound and histology evaluation of a novel fully bioabsorbable poly-L-lactic acid/amorphous calcium phosphate scaffolds in porcine coronary arteries," *Journal of Biomedical Nanotechnology*, vol. 12, no. 4, pp. 743–752, 2016.

[8] D. Gu, G. Feng, G. Kang et al., "Improved biocompatibility of novel biodegradable scaffold composed of poly-L-lactic acid and amorphous calcium phosphate nanoparticles in porcine coronary artery," *Journal of Nanomaterials*, vol. 2016, Article ID 2710858, 8 pages, 2016.

[9] X. Zheng, Y. Wang, Z. Lan et al., "Improved biocompatibility of poly(lactic-co-glycolic acid) and poly-L-lactic acid blended with nanoparticulate amorphous calcium phosphate in vascular stent applications," *Journal of Biomedical Nanotechnology*, vol. 10, no. 6, pp. 900–910, 2014.

[10] Z. Lan, Y. Lyu, J. Xiao et al., "Novel biodegradable drug-eluting stent composed of poly-L-lactic acid and amorphous calcium phosphate nanoparticles demonstrates improved structural and functional performance for coronary artery disease," *Journal of Biomedical Nanotechnology*, vol. 10, no. 7, pp. 1194–1204, 2014.

[11] J. Xiao, G. Feng, G. Kang et al., "6-month follow-up of a novel biodegradable drug-eluting stent composed of poly-L-lactic acid and amorphous calcium phosphate nanoparticles in porcine coronary artery," *Journal of Biomedical Nanotechnology*, vol. 11, no. 10, pp. 1819–1825, 2015.

[12] H. Li, K. Sun, R. Zhao et al., "Inflammatory biomarkers of coronary heart disease," *Frontiers in Bioscience*, vol. 10, pp. 185–196, 2018.

[13] J. D. Beck, K. L. Moss, T. Morelli, and S. Offenbacher, "Periodontal profile class is associated with prevalent diabetes, coronary heart disease, stroke, and systemic markers of C-reactive protein and interleukin-6," *Journal of Periodontology*, vol. 89, no. 2, pp. 157–165, 2018.

[14] L. Chen, H. Deng, H. Cui et al., "Inflammatory responses and inflammation-associated diseases in organs," *Oncotarget*, vol. 9, no. 6, pp. 7204–7218, 2018.

[15] C. S. Hansen, D. Vistisen, M. E. Jørgensen et al., "Adiponectin, biomarkers of inflammation and changes in cardiac autonomic function: Whitehall II study," *Cardiovascular Diabetology*, vol. 16, no. 1, p. 153, 2017.

[16] I. Ragino, A. M. Cherniavskiĭ, I. Polonskaia et al., "Inflammatory-destructive biomarkers of atherosclerotic plaques instability. Study of arterial wall and blood," *Kardiologiia*, vol. 52, no. 5, pp. 37–41, 2012.

[17] G. Feng, C. Qin, X. Yi et al., "Effect of novel bioresorbable scaffold composed of poly-L-lactic acid and amorphous calcium phosphate nanoparticles on inflammation and calcification of surrounding tissues after implantation," *Journal of Materials Science: Materials in Medicine*, vol. 29, no. 8, p. 112, 2018.